

Calspan

*THE EFFECT OF FRAME PROPERTIES
ON BICYCLING EFFICIENCY*

Task Order No. 6

J.A. Davis and R.J. Cassidy

Calspan Report No. ZN-5431-V-2

Prepared For:

SCHWINN BICYCLE COMPANY
CHICAGO, ILLINOIS

NOVEMBER 1974

This report has been reviewed and approved by:

A handwritten signature in black ink that reads "E. A. Kidd". The signature is written in a cursive style with a large initial "E" and a long, sweeping underline.

E. A. Kidd, Head
Transportation Safety Department

TABLE OF CONTENTS

	<u>Page</u>
1.0 INTRODUCTION	1
2.0 ENERGY USE IN BICYCLING	2
3.0 THE ROLE OF THE FRAME IN ENERGY USE	5
4.0 COMPARATIVE FRAME TESTS	17
5.0 CONCLUSIONS AND RECOMMENDATIONS	30

1.0 INTRODUCTION

In a previous study for Schwinn, Calspan investigated bicycling energy requirements as a function of velocity, road grade, tire properties, and other factors, including rider/bicycle weight. Tire construction and stiffness were shown to have significant effects on level road energy requirements over a wide range of speeds. Except for the inclusion of certain tire properties, however, the bicycle model used in this study was assumed to be a perfectly rigid body.

The objective of the study discussed herein was to begin to define and explore the effect of frame properties on the energy requirements of bicycling. A thorough study of this subject would require the investigation of frame construction and materials, frame reaction to static and dynamic loading and the many physiological factors which define the rider's application of forces to the bicycle.

In this initial treatment of the subject, we first describe the various modes of energy use in bicycling and show which of these may be affected by frame properties. Of particular interest is the extent to which frame flexure under pedalling loads is responsible for non-propulsive energy consumption. This point is of considerable significance since it directly relates to the task of designing frames for maximum energy utilization. Under a set of assumed conditions, we have begun to analyze the mechanism of energy consumption through frame flexure.

An experimental phase of this effort was devoted to obtaining data on the relative stiffness of three frames of different construction and material which were provided by Schwinn. Hysteresis curves were obtained for each frame under typical loading conditions which relate applied forces to the resultant deflections, and provide both stiffness information and also an insight into energy absorption due to frame flexibility. The corresponding front forks were tested separately to provide data which may later be used to relate fork flexibility to high speed weave oscillations.

2.0 ENERGY USE IN BICYCLING

Our chief objective in this study was to relate the physical properties of bicycle frames to their efficiency in transferring input energy at the pedal to tractive energy at the rear wheel. Naturally, other components of the bicycle will also participate in and affect this energy transfer, but the present effort is limited to study of the frame alone. In fact, conclusions can be drawn about the effect of some of these other components by analogy with frame properties.

The first step in the analysis of frame effects on energy consumption was to define the areas of energy use in bicycling and decide where in this classification could be placed the energy that went into flexing the frame during pedalling. More important, however, was determining how this energy was dissipated. If, in fact, the energy required to deform the frame was eventually transferred into tractive energy when the frame was unloaded, then no loss of pedal input energy had occurred due to frame deflection. This theory, though, does not agree with the widely held belief that stiff bicycles are more efficient than flexible ones. It also assumes the fact that the frame is completely elastic.

Figure 1 presents a simple classification of ways in which energy is consumed during bicycling along a straight, level path. First of all, energy will be lost through friction in the drive system and bearings as well as through tire flexing. Also, any roll accelerations of the bicycle and rider caused by off-center pedal forces will consume energy. "Propulsion" includes all the input energy required to accelerate the bicycle/rider system and overcome rolling resistance and aerodynamic drag.

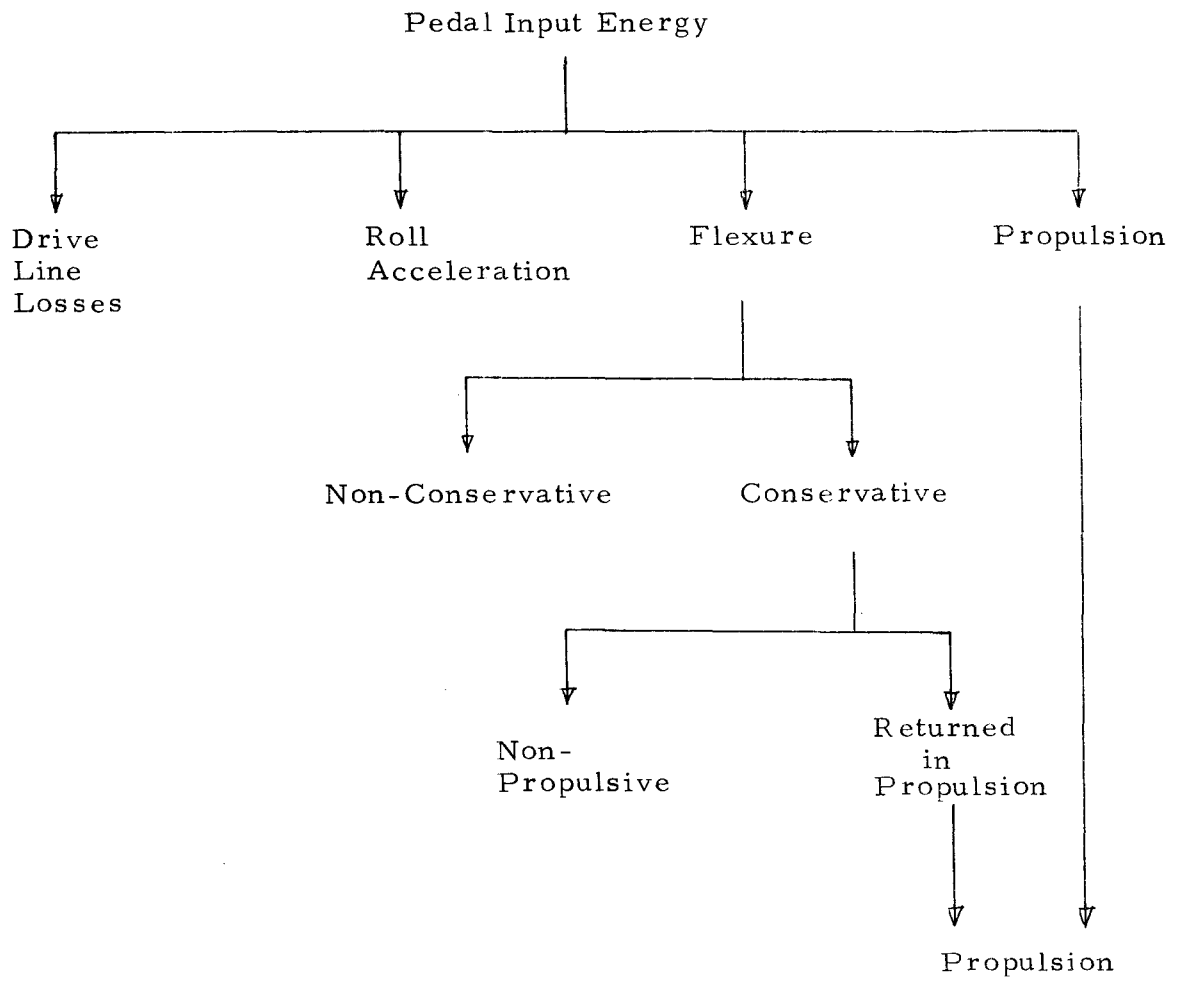


FIGURE 1 AREAS OF ENERGY USE

Of most concern to us here is the energy which goes into flexure, and the ultimate result of that energy. This energy falls into two categories, conservative and non-conservative. In this case, the non-conservative energy is taken to mean that which results in the generation of heat in the frame due to bending. As we will show later, this constitutes a negligible portion of the total flexure energy.

"Conservative" energy is defined as conservative with respect to the bicycle itself and is not reflected as heat generated in the frame. This energy can be compared to that arising when a man pushes back and forth on a perfectly elastic spring having no damping (a conservative spring) at a very slow rate so that inertia forces (and consequently resonance) are not involved. In this case, no energy is lost in the spring. Zero total work is done on the spring, and zero total work is done by (and on) the man. That is, positive work is done on the spring in the forward push, and equal and opposite work is done by the spring in the extension portion of the stroke. Though the energy applied from spring to man is zero, the man obviously expends a net amount of energy; in fact, he may expend about as much energy in the extension portion of the stroke as in the compression portion. Thus, we are dealing with energy losses associated with the fact that the man is not a conservative system; the man is not able to convert any of the work applied to him in the extension stroke to work applied back to the spring in the compression stroke.

This analogy falls short of describing the man/bicycle system, since some of the conservative flexure energy associated with the deflection of the bicycle frame under pedalling load is returned as useful tractive energy, while the remainder is an actual energy loss due to the non-conservative nature of the man, as in the man/spring system. We will describe these two types of conservative flexure energy as that which ultimately results in propulsion and that which is non-propulsive. How much of each type occurs depends on how the rider applies energy to the bicycle and the reaction of the frame to the applied force. These topics will be discussed further in the following section.

3.0 THE ROLE OF THE FRAME IN ENERGY USE

Before analyzing the effects of frame deflection on energy expenditure, it is necessary to describe the static force balance of the rider/bicycle system. Three possible static balances of the bike under forces applied from the rider are shown below. The static weight of the rider is neglected in all cases, because our concern here is the reaction of the frame in pedalling. The conclusions reached in this analysis will not be compromised by this simplifying assumption.

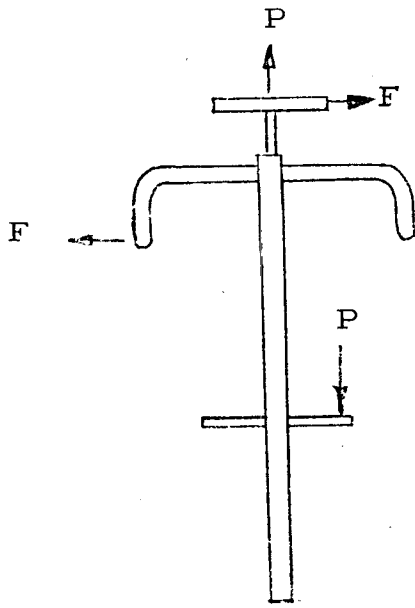


FIGURE 2a

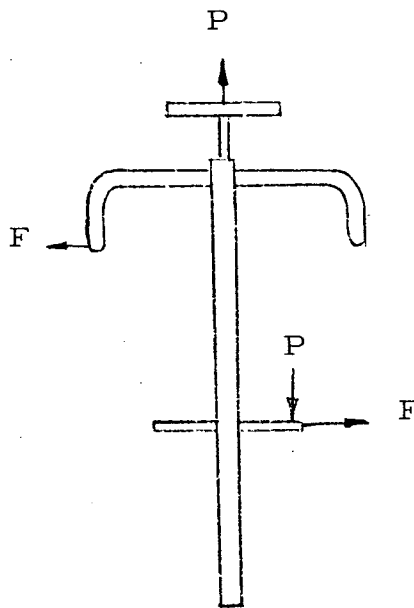


FIGURE 2b

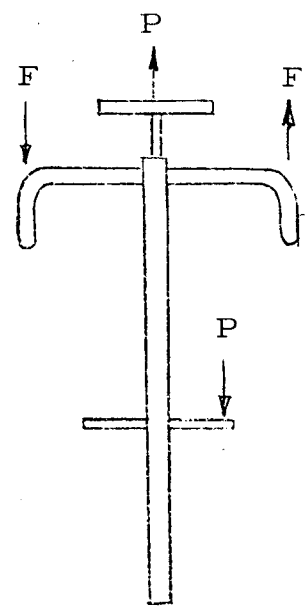


FIGURE 2c

In case (a) the rider applies a pedal force P which is reacted by an equal and opposite reduction in vertical force between the rider and the bike seat. The couple produced by the P forces is reacted by a horizontal force couple at the handlebar and seat. The lateral force (F) will reverse in direction as dominant pedal force changes from side to side, causing oscillating lateral motions for bike and rider. These motions would not occur in case (b) where the lower reacting couple force acts at the pedals (a lateral force between the rider's foot and the pedals) instead of at the ground. In case (c), the moment reacting forces are at the handlebar. Case (c) evidently represents the most severe case, because the full moment resulting from off center pedal force acts through the entire frame; in cases (a) and (b) this moment reduces from a maximum value at the level of the pedals to zero at the handlebar. In the discussion and analysis to follow we consider the most severe case (c). Moreover, case (c) most accurately represents the true force balance, particularly in cases of high pedal force such as in hill climbing. This is especially true when the high pedal force is applied at low speeds, for the roll moment due to the pedal force is reacted by the rider most naturally by an upward force on the handlebar on the same side as the pedal force.

Representation of Frame Flexibility

All of the frame elements connecting the crank shaft to the seat, handlebar and wheel bearings have continuous flexibility along their lengths. However for purposes of investigating the effect of frame flexibility on energy losses and tractive energy, it is convenient to represent frame flexibility by lumped springs as shown below.

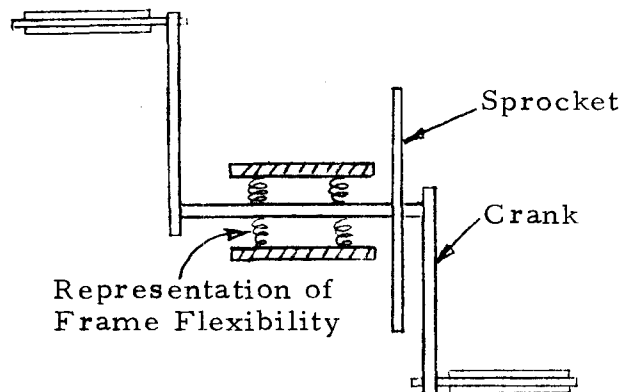


FIGURE 3

For the loads applied in Figure 2c, the two effective springs shown in Figure 3 can be used to represent vertical and moment frame flexibility. Load P applied to the pedals causes vertical and rotational motions of the crankshaft assembly in the roll plane, which is the plane of Figure 3. These motions, in turn, cause rotation of the sprocket and ultimately tractive force at the rear wheel. The relationship between frame flexibility, crankshaft motions, sprocket driving motions, and corresponding spring energy and traction energy is investigated below.

Relationship Between Pedal Forces, Frame Deflections, Tractive Energy and Spring Energy

Figure 4a shows the vertical deflection and rotation of the crankshaft in the roll plane caused by the application of the pedal force.

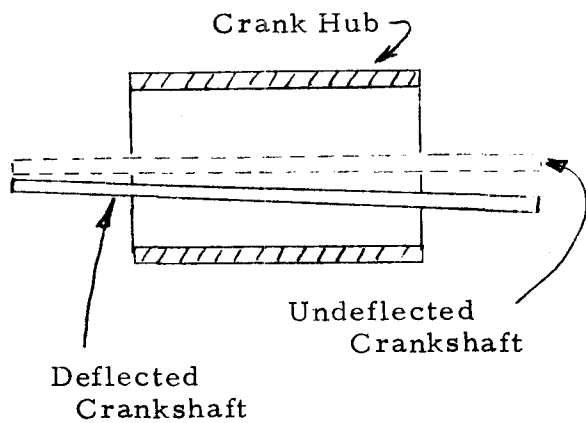


FIGURE 4a FRONT VIEW

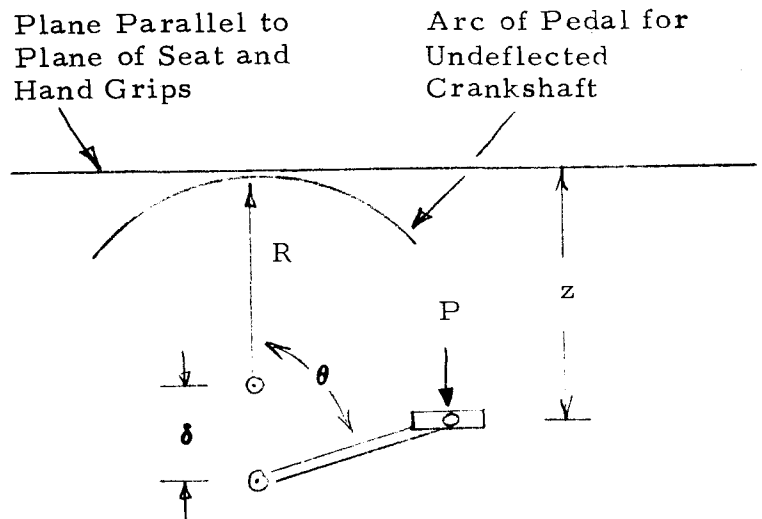


FIGURE 4b SIDE VIEW

It is assumed that the rider maintains the handlebar in a level position. Thus, the rotation of the crankshaft in the roll plane occurs with respect to fixed handlebar position and fixed ground position. From Figure 2, the vertical reaction to the pedal force occurs as an upward load at the seat, causing the effective spring extension of the bike frame to occur between the crankshaft and the plane defined by the seat and hand grips. In calculating crankshaft motions in Figures 4a and 4b, we consider this plane to be the fixed frame of reference, though it actually undergoes vertical and pitch motions with respect to the ground. Since the rider moves with this plane, selection of this plane as the reference permits the necessary analysis of crank motions and crankshaft motions with respect to the rider's foot.

From inspection of Figure 4b, the deflection (z) of the pedal with respect to a plane parallel to the plane of reference (and passing through the apex of the arc formed by the pedal rotating about an undeflected crankshaft) is given by

$$z = \delta + R - R \cos \theta \quad (1)$$

where δ is the deflection at the crank point of rotation due to frame flexibility, and θ is the crank rotation angle. Since the stresses in the bike frame are assumed to be in the elastic (linear) range, the deflection δ can be expressed as follows

$$\delta = \frac{P}{k} \quad (2)$$

where P is the vertical load applied at the pedal, and reacted by the frame, and k is a constant determined by frame stiffness. Substituting (2) into (1),

$$z = \frac{P}{k} + R - R \cos \theta \quad (3)$$

We are interested in analyzing a situation where the pedal load P is defined with respect to pedal vertical position. A typical force-deflection curve is shown below.

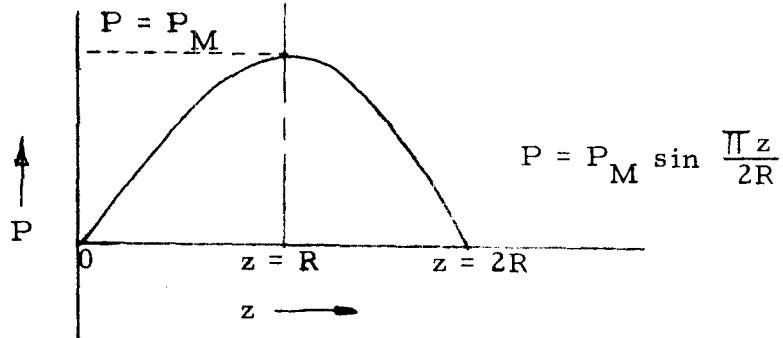


FIGURE 5

For the sine curve, P is given by

$$P = P_M \sin \frac{\pi z}{2R} \quad (4)$$

The peak of the sine curve occurs at

$$\frac{\pi z}{2R} = 90^\circ = \frac{\pi}{2} \quad (5)$$

from which z corresponding to maximum pedal force is equal to crank radius R . Enforcing this condition ($P = P_M$ at $z = R$) in equation 3, we obtain

$$\theta_{P_M} = \cos^{-1} \frac{P_M}{kR} \quad (6)$$

where θ_{P_M} is the crank angle at the instant when the pedal force is maximum. For the case of an infinitely rigid frame ($k = \infty$) equation (6) shows that the force-deflection curve of Figure 5 results in a crank angle of 90° at maximum pedal force P_M . However, for finite amounts of frame stiffness, the crank angle is less than 90° by an amount depending on frame stiffness k . This lag in crank angle is equal to

the lag in sprocket angle (assuming the crankshaft and sprocket are rigid) and is evidently associated with a reduction in propulsive energy (from the perfectly rigid frame case) equal to the amount of energy stored in the spring. The spring energy at maximum pedal force where $P = P_M$ is given by

$$E = \frac{1}{2} k \delta^2 = \frac{P_M^2}{2k} \quad (7)$$

That the cumulative energy lost in propulsion at any given time is, in fact, equal to the energy stored in the spring can be verified by integrating the force/deflection curve produced by the rider, and subtracting from this the integrated torque versus θ curve produced at the sprocket. The energy which has been delivered from the rider to the bike at the instant of maximum pedal force in Figure 5 is given by

$$E_R = \int_{z=0}^{z=R} P_M \sin \frac{\pi z}{2R} dz \quad (8)$$

This is equal to

$$E_R = -P_M \left[\frac{2R}{\pi} \right] \cos \frac{\pi z}{2R} \Bigg|_{z=0}^{z=R} \quad (9)$$

from which

$$E_R = 2 \frac{P_M R}{\pi} \quad (10)$$

The energy which has been directly converted to propulsion in this same time period is given by

$$E_T = \int_{\theta=0}^{\theta = \cos^{-1} \frac{P_M}{kR}} T d\theta \quad (11)$$

where T is the torque delivered by the crank to the sprocket. From Figure 4b, this torque can be expressed as

$$T = PR \sin \theta \quad (12)$$

Substituting expression (12) for T and expression (4) for P into equation (11), we obtain

$$E_T = \int_{\theta=0}^{\theta=\cos^{-1} \frac{P_M}{kR}} P_M \sin \frac{\pi z}{2R} R \sin \theta \, d\theta \quad (13)$$

The integration in equation 13 must be performed in a single variable. By substituting expression (4) for P into equation 3, we obtain the following relationship between z and θ .

$$z = \frac{P_M}{k} \sin \frac{\pi z}{2R} + R - R \cos \theta \quad (14)$$

Differentiating equation (14) and transposing terms, we obtain

$$R \sin \theta \, d\theta = dz \left\{ 1 - \left[\frac{P_M}{k} \right] \frac{\pi}{2R} \cos \frac{\pi z}{2R} \right\} \quad (15)$$

Inserting this expression for $R \sin \theta \, d\theta$ into equation (13), we obtain

$$E_T = \int_{z=0}^{z=R} \left[P_M \sin \frac{\pi z}{2R} - \frac{P_M^2}{k} \frac{\pi}{2R} \sin \frac{\pi z}{2R} \cos \frac{\pi z}{2R} \right] dz \quad (16)$$

The second term in (16) is simplified by noting that

$$\sin \frac{\pi z}{2R} \cos \frac{\pi z}{2R} = \frac{1}{2} \sin \frac{\pi z}{R} \quad (17)$$

Inserting (17) into (16) and performing the integration, we obtain

$$E_T = - P_M \frac{2R}{\pi} \cos \frac{\pi z}{2R} \Bigg|_{z=0}^{z=R} + \frac{P_M^2}{k} \frac{1}{4} \cos \frac{\pi z}{R} \Bigg|_{z=0}^{z=R} \quad (18)$$

from which

$$E_T = P_M \frac{2R}{\pi} - \frac{P_M^2}{2k} \quad (19)$$

If this expression for propulsive energy is subtracted from expression (10) for total energy delivered to the bike by the rider, the remainder is simply

$$E_N = \begin{array}{l} \text{Energy not directly} \\ \text{delivered to propulsion} \end{array} = \frac{P_M^2}{2k} \quad (20)$$

Comparison with expression (7) for frame spring energy verifies that the portion of total energy not delivered to propulsion is exactly equal to frame spring energy. Though this calculation was made for a particular level of pedal force (P_M) on a particular pedal force versus deflection curve (given by Figure 5), investigation of other pedal force versus deflection curves and other force levels will verify that the cumulative energy lost to propulsion is equal at any instant to the energy stored in the spring, provided that the force/deflection curve applied by the rider to the bike goes through zero at the minimum and maximum deflection points, as is the case in Figure 5.

Before investigating the situation for force/deflection curves which do not meet this condition, it is well to summarize the meaning of the results obtained so far. For all pedal force deflection curves which go through zero at the deflection extremities, any energy which is lost in frame deformation at a particular instant is subsequently recovered fully in the form of propulsive energy, since the instantaneous spring energy, and therefore the cumulative energy lost in propulsion, returns to zero at every half cycle of the rider's force deflection curve. The only qualifications to this conclusion arise from conditions previously stated, specifically:

- that the forces between rider and bike are as shown in Figure 2c
- that energy lost in the form of heat in the frame material is neglected.

The amount of propulsive energy losses occurring when these restrictions are not applied will be investigated separately.

A significant characteristic of the flexible bike is that unloading of the effective frame spring causes propulsive forces. An explanation of the physical mechanism is as follows. Consider a rider starting at the origin of the force/deflection curve in Figure 5. He applies force to the pedal, developing tractive forces at the rear wheel. This is done very slowly so that inertia forces are not involved. At some point on the force/deflection curve, (say the peak of the curve) both rider and driving wheel are simultaneously locked in position. The wheel is prevented from rotating in its plane, and the driver is fixed with respect to the reference plane determined by the seat and hand grips. In this locked position of rider and bike, the frame is deformed so that the crankshaft is deflected with respect to the reference plane, as shown in Figure 4a. We now release the constraint on the driving wheel, but do not release the constraint on the rider. At this time, the effective springs act to restore the crankshaft from its deflected position shown in Figure 4a to its original

undeflected position. Thus, in Figure 4b, the center of rotation of the pedal crank moves upward by an amount δ to its initial undeflected position. However, since the rider is held fixed with respect to the reference plane (which is free to move with the bike) the vertical location of the pedal remains in the position shown in 4b. It can be seen from the figure that this constraint, in combination with the vertical motion δ at the crank center, produces a rotation of the crank and sprocket. This will cause rotation of the driving wheel and development of a tractive force which propels rider and bike forward. Thus, given that the position of the rider's foot is defined, unloading of the spring causes rotation at the sprocket and development of traction at the driving wheel.

The mechanism described above does not apply when the crank is in the vertical position, whether full upward or full downward. If the rider initially applies pressure to the pedal in the full downward position, for example, the only result will be a deflection δ at the pedal. Releasing of the force will permit the frame to return to its undeflected position with no driving motion imparted to the crankshaft. This is exactly the same as the case of the man pushing against a spring. Zero net work is done on the spring (frame), but the rider has expended energy because he does not represent a conservative system. Further, for the family of hypothetical force deflection curves shown in Figure 6a, the same mechanism applies. For these curves, a portion of the load is applied in the full upward position of the pedal, and remains on the pedal to the full downward position, where it is released. The loading and unloading of the spring which occurs in the full up and full down positions does not influence propulsion, and constitutes wasted energy for the rider, up to a maximum possible level of twice the energy stored in the spring when the pedal reaches the full down position.

The force deflection curves in Figure 6a would not occur in practice, since they require a step change in pedal load in the full down position.

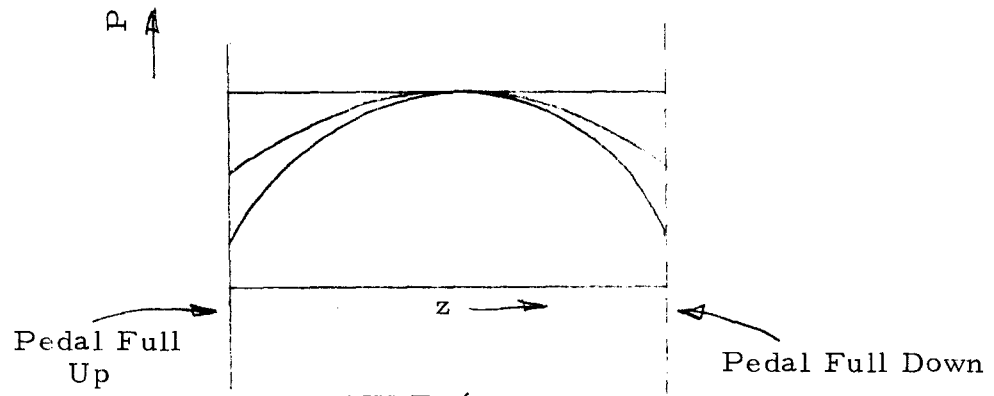


FIGURE 6a

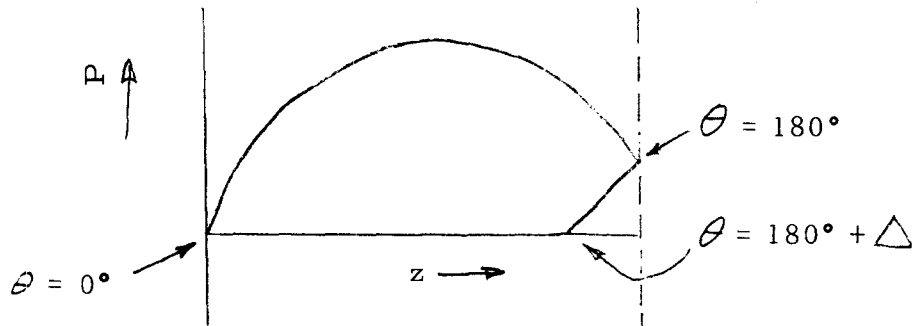


FIGURE 6b

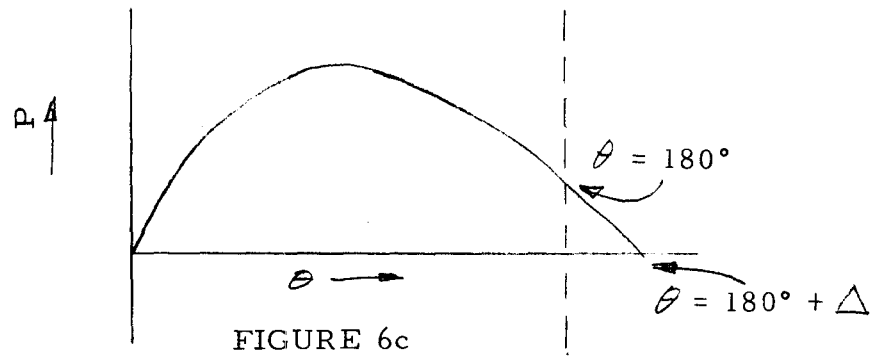


FIGURE 6c

However, it is apparently possible for a force-deflection characteristic such as that shown in Figures 6b and 6c to occur in practice. These two figures reflect the same rider force input, Figure 6b showing force versus deflection and Figure 6c showing force versus crank angle. In this case, wasted rider energy could also approach a maximum of twice the energy stored in the spring when the full down position is reached. This factor of two arises from (1) the energy stored in the spring when the pedal reaches the full down position plus (2) the fact that spring unloading in crank positions past 180° provides negative driving energy because it acts to reduce crank angle. Furthermore, a more flexible frame will undergo a greater deflection under a given force and return its spring energy over a longer period of time after the force is removed. The further this occurs after 180° , the greater will be the effective crank arm length and the greater will be the retarding torque that is applied.

In this analysis we have considered how pedal force energy stored in the frame through flexure can be returned as useful tractive energy. However, there is a further means other than those discussed by which significant amounts of stored frame energy might be lost. If the rider inputs a force which is normal to the plane of the front sprocket, then the energy stored due to resultant deflection of the frame will be returned with no force component to cause sprocket rotation, and thus will provide no useful tractive energy. This is closely analogous to the man/spring system discussed previously. The imposition of a lateral force by a rider might be caused by a severe deformation of the frame under load and in this way could be related to frame flexibility.

4.0 COMPARATIVE FRAME TESTS

A major objective of this work was the investigation of the physical properties of frames which could be correlated to their energy efficiency under load. For this effort, Schwinn provided the following three frames, which represent different materials and construction methods:

- Continental (welded low carbon steel)
- Super Sports (welded chrome molybdenum steel)
- Paramount (lug joined Reynolds 531 double butted tubing)

The same tests were run on each frame and were designed to provide information comparing the relative stiffness of each frame and the degree to which each would dissipate energy as heat generated due to flexure. Typical loads were applied to the frame and both applied force (F) and deflection (δ) were measured during the application and release of the load. A BLH Model No. (03G1) load cell was used to measure force and two different types of displacement transducers were used to measure deflection. The signals were amplified and displayed on a Tectronix type 564 storage oscilloscope with force on the "y" axis and deflection on the "x" axis. The resultant force/deflection curves were used to determine frame stiffness and hysteresis energy losses. In each case, the force was applied slowly (over a period of 3-10 seconds) so that it could be considered as a static load.

As mentioned before, we chose to test the forks and frames separately to simplify the analysis of their properties. In an initial study such as this one, it was thought that testing the fork and frame separately would yield more useful information.

Figures 7a and 7b show the test setup for the measurement of fork properties. Force was applied laterally along the front hub axis up to a maximum load of 50 pounds, which was considered to be the maximum lateral load imposed on the fork during normal bicycling maneuvers. The lateral load condition was selected for investigation because of its implications in handling phenomena, such as the high speed weave oscillation. Deflection was measured

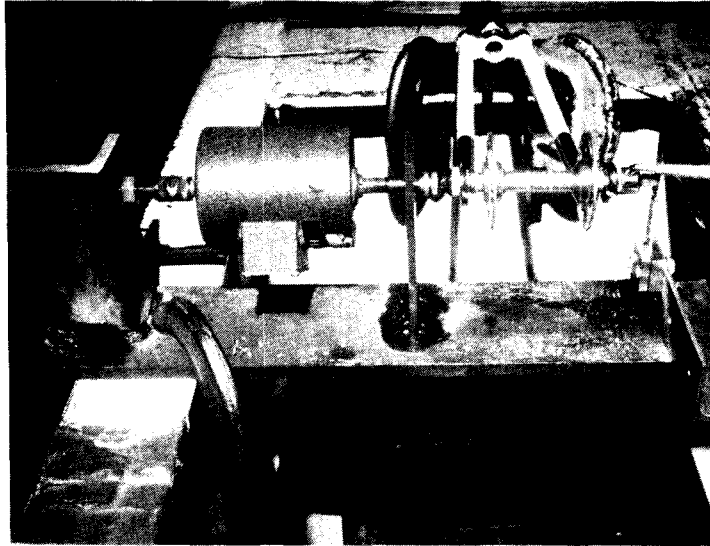


FIGURE 7a

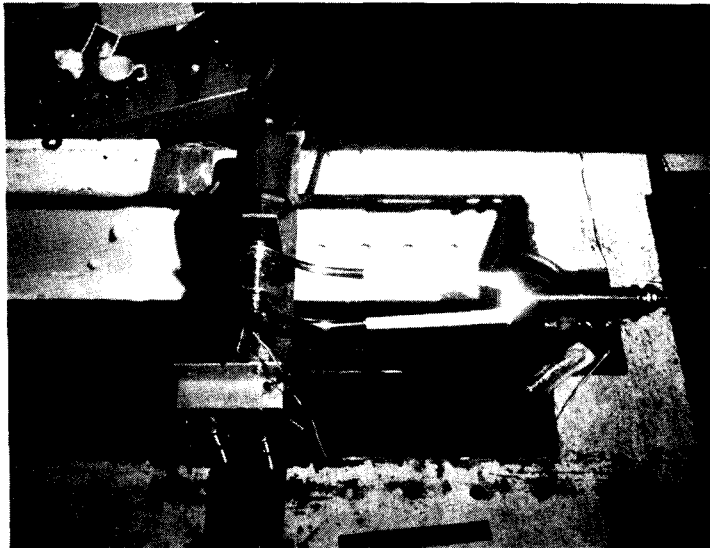


FIGURE 7b

FRONT FORK LATERAL LOAD TESTS

by a thin steel flexure to which a set of strain gages was bonded. This appears at the right of the hub in Figure 7a.

The force/deflection curves for the Super Sports fork and the Paramount fork are shown in Figures 8 and 9, respectively. (The data for the Continental fork was not taken; it was at first assumed that the Continental and Super Sports forks were identical, since they were not described separately on the shipping invoice. After the fork tests the dimensions of the two forks were discovered to be different.) The lateral stiffness of the Super Sports fork (294 lbs/in) is only slightly less than that of the Paramount (318 lbs/in).

Earlier in our discussion we drew certain conclusions regarding spring energy of the frame and qualified them by stating that they neglected heat energy losses incurred in flexure. In both these cases, this seems to be a valid assumption, since the F/δ traces for the application and release of the applied force are coincident, indicating little or no energy loss in flexure. The energy input for maximum deflection ($\delta = \delta_m$) is given by

$$E = \int_0^{\delta_m} F(\delta) d\delta \quad (21)$$

which in this case, where $F(\delta) = k\delta$, reduces to

$$E = \int_0^{\delta_m} k\delta d\delta = \frac{1}{2} k\delta_m^2 \quad (22)$$

which is the same expression as equation (7) for the frame spring energy at maximum pedal force. If, as in the case of these two forks, the F/δ curve representing the release of the force follows the application curve, then the heat energy loss (E_H) is given by

$$E_H = \int_0^{\delta_m} k\delta d\delta - \int_{\delta_m}^0 k\delta d\delta = 0 \quad (23)$$

If the F/δ curve upon release fell below the application curve, then $F(\delta) \neq k\delta$ and the energy returned by the fork after release,

$$E_{\text{released}} = \int_{\delta_m}^0 F(\delta) d\delta$$

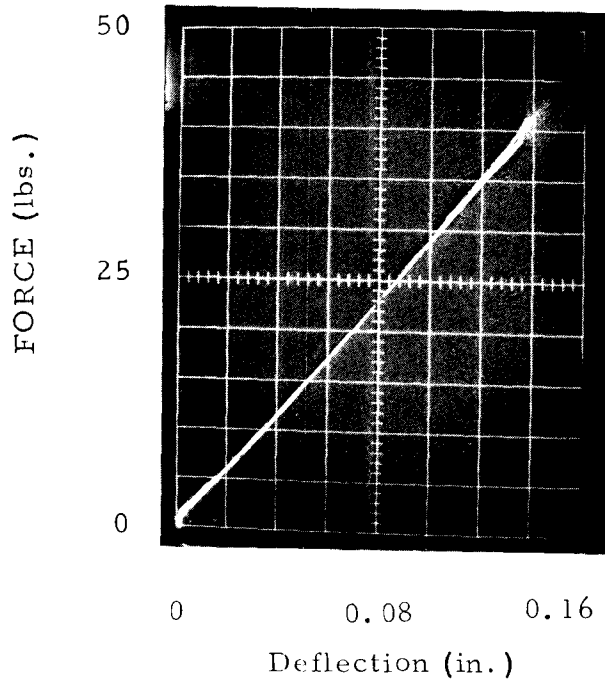


FIGURE 8 SUPER SPORTS FORK
294 lbs/in

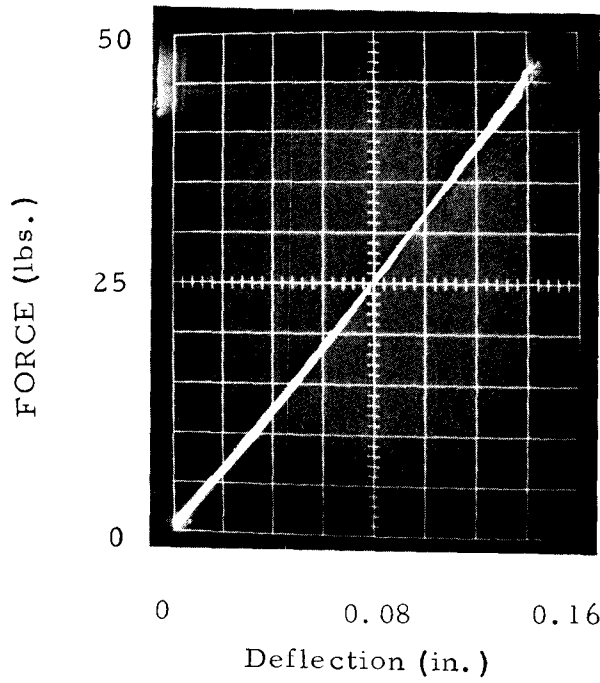


FIGURE 9 PARAMOUNT FORK
318 lbs/in

would be less the input energy of equation (22) and net energy loss to heat would be indicated.

At the maximum deflection point of Figures 8 and 9, the application and release curves separate slightly and are joined by a short vertical line. This does not represent energy loss in the fork, but rather friction in the fixtures used to mount the load cell and apply the force. This problem is more apparent in the frame test data which follow.

Two different tests were performed on each of the three frames to characterize their reactions to loading. The first was a lateral load test in which the force was applied by an hydraulic cylinder at the crank hub in the direction of the crank axis. This test setup is shown in Figures 10a-d. To eliminate the effect of the fork, the frame was connected at the headtube to a 4" x 4" steel tube which acted as a relatively inflexible "virtual" fork which pivoted about an axis coincident with the front hub axis. The frame was free to rotate about the steer axis under load. To simulate the effects of a rear wheel and tire, the rear dropouts were mounted on a shaft which was supported by a spherical bearing as shown in Figure 10d. For each of the frame tests, deflection was measured with the linear potentiometer shown in Figure 10c.

The results of this test using the three frames are shown in Figures 11, 12 and 13. Here again, the vertical line at maximum deflection represents the force required to overcome the various sources of friction in the loading fixture. Since this frictional force occurs in both loading and unloading, the vertical line represents twice the force and thus the frictionless force/deflection curve would pass through its midpoint. That point is used to calculate the following stiffness values:

Continental	252 lbs/in
Super Sports	237 lbs/in
Paramount	171 lbs/in

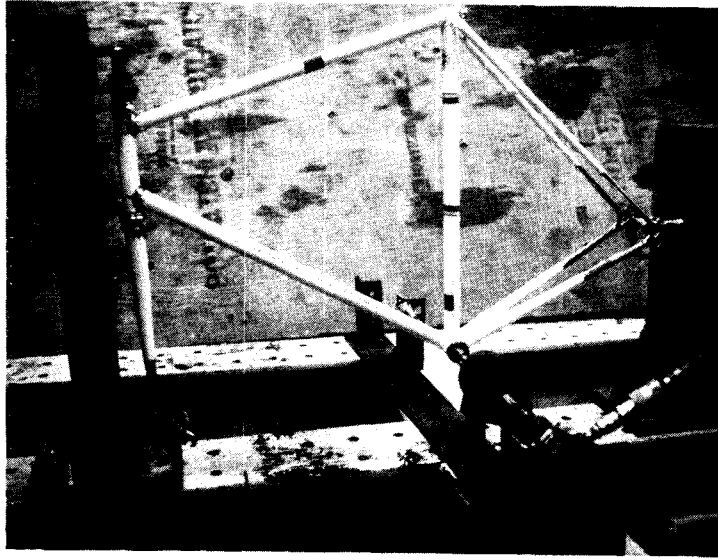


FIGURE 10a

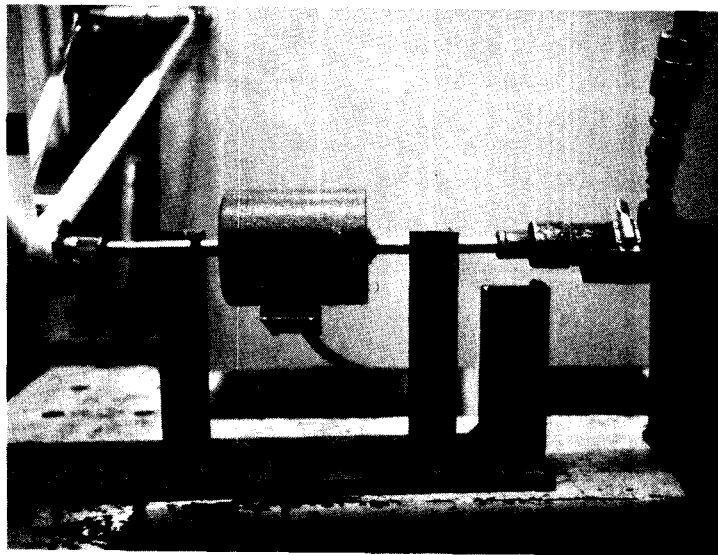


FIGURE 10b

FRAME LATERAL LOAD TESTS

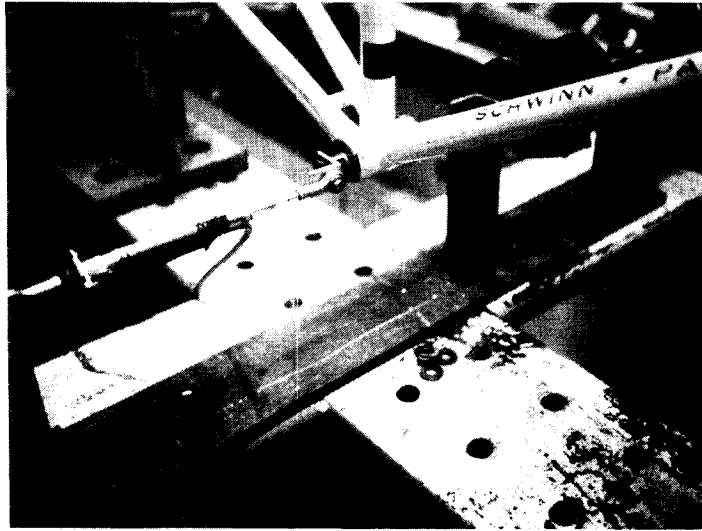


FIGURE 10c

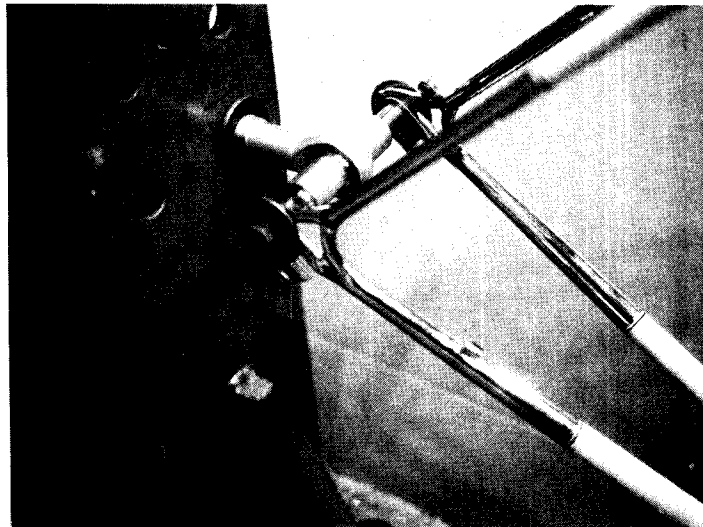


FIGURE 10d

FRAME LATERAL LOAD TESTS

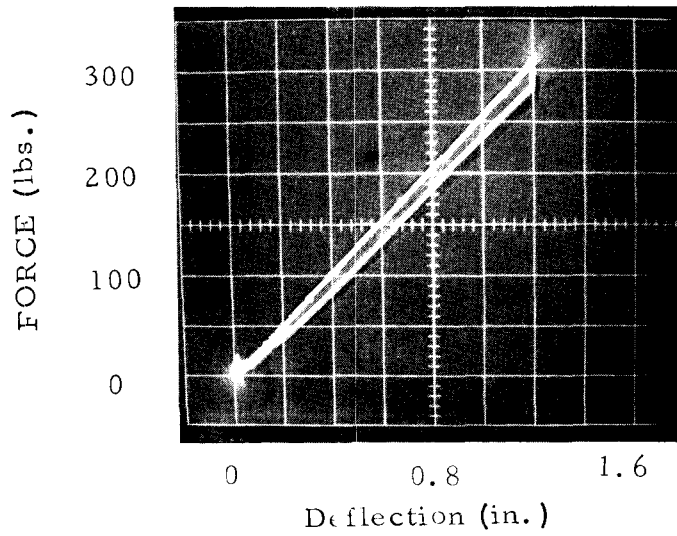


FIGURE 11
CONTINENTAL FRAME
LATERAL LOAD
252 lbs/in

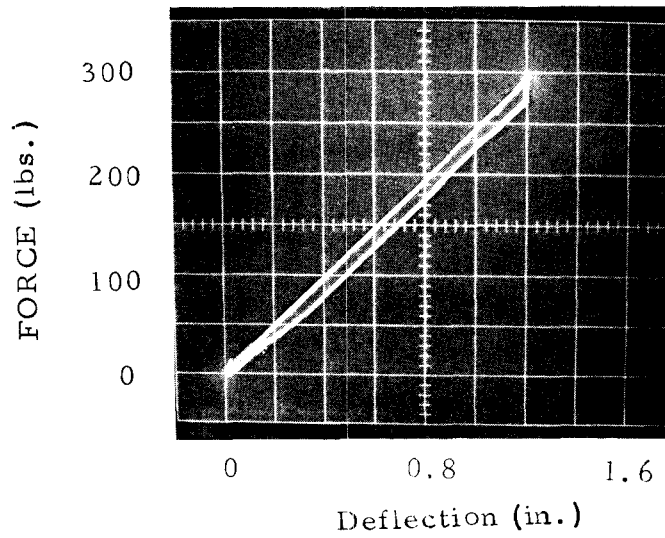


FIGURE 12
SUPER SPORTS FRAME
LATERAL LOAD
233 lbs/in

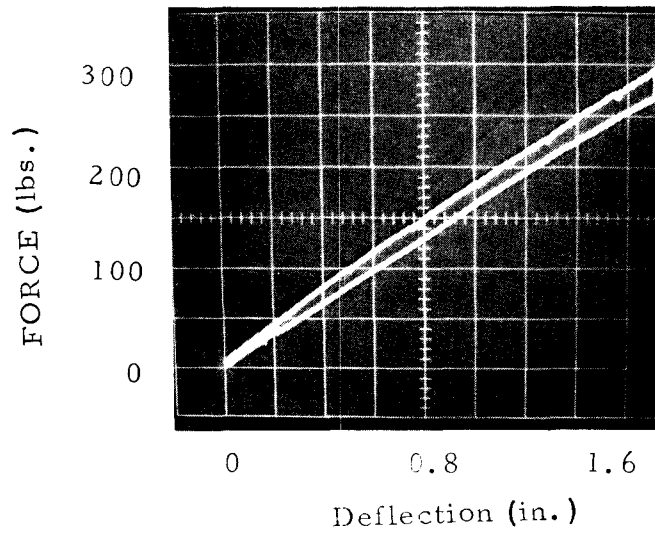


FIGURE 13
PARAMOUNT FRAME
LATERAL LOAD
171 lbs/in

The Continental and Super Sports frames are not greatly different, but the Paramount is a good deal more flexible than expected. The Paramount frame also exhibits a slightly non-linear force/deflection curve for which we have no adequate explanation at this time. The large amount of friction in the fixtures used for this test unfortunately cloud the analysis of frame energy losses due to heat. It does seem, however, that the areas between the application and release curves show little or no difference among the three cases, implying that the energy utilization of each frame is about equal.

The remaining frame test was done under conditions more closely simulating the loads the frame will encounter during bicycling. As shown in Figures 14a and b, a thick-walled tube was inserted into the crank hub and a vertical force was applied to a plate on the end of this tube, simulating pedal force. This fixture was used so we could analyze the effect of the force and moment induced by pedal force without including the effects of pedal and crank deflection. The distance from the center of the hub to the center of the pedal is 5.28" for the Continental and Super Sports, but 4.78" for the Paramount. To provide consistent data, all three frames were tested with the application point of the pedal force placed 5.00" from the hub center.

For the pedal force tests, the frames were mounted differently than they were in the lateral force tests. To simulate real-world conditions, it was necessary to allow the frame freedom to deflect along its longitudinal axis, so the virtual fork was supported on two roller bearings resting on a flat surface. Also, the rear dropouts were rigidly attached to the test fixture support.

For this series of tests, both vertical and lateral deflections of the virtual pedal were measured. The results are shown in Figures 15 and 16 and stiffness coefficients are summarized below:

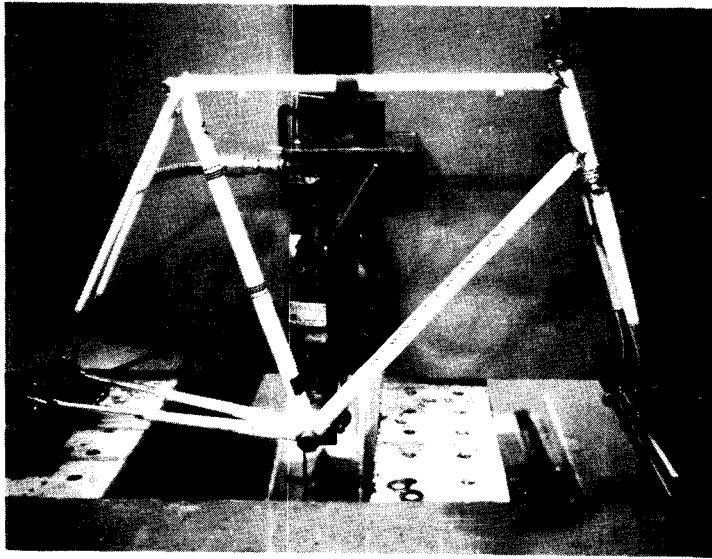


FIGURE 14a

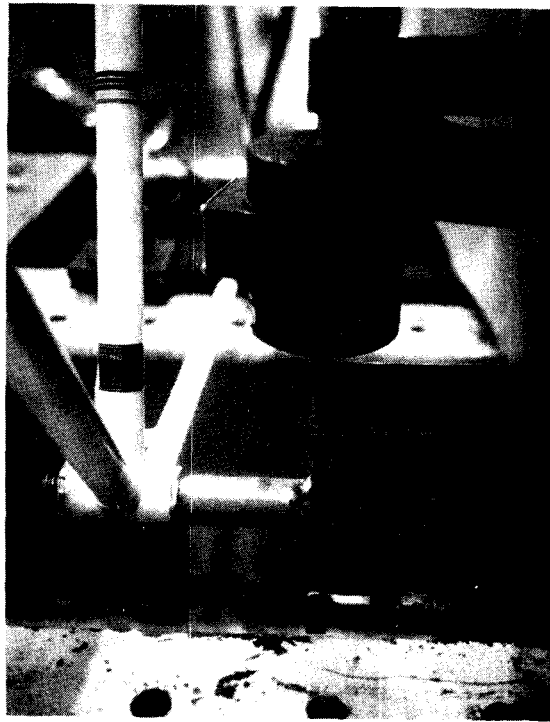


FIGURE 14b
FRAME PEDAL LOAD TESTS

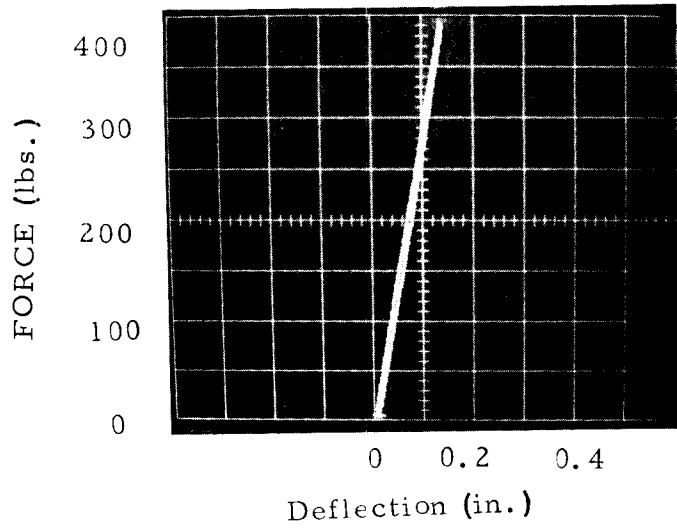


FIGURE 15a
CONTINENTAL
FRAME
2900 lbs/in

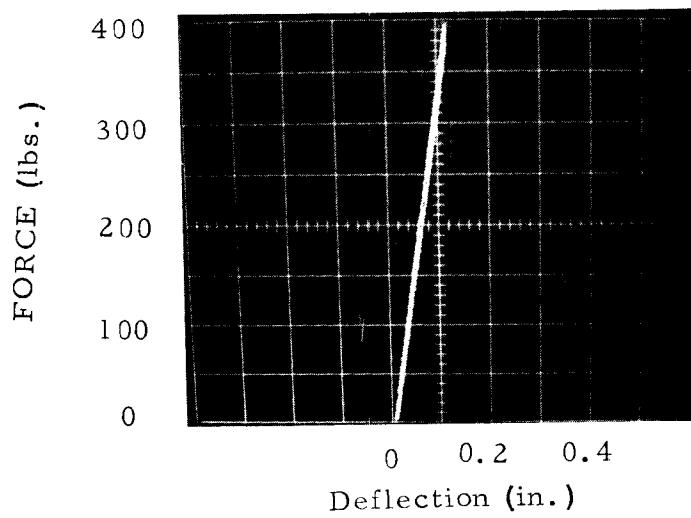


FIGURE 15b
SUPER SPORTS FRAME
3300 lbs/in

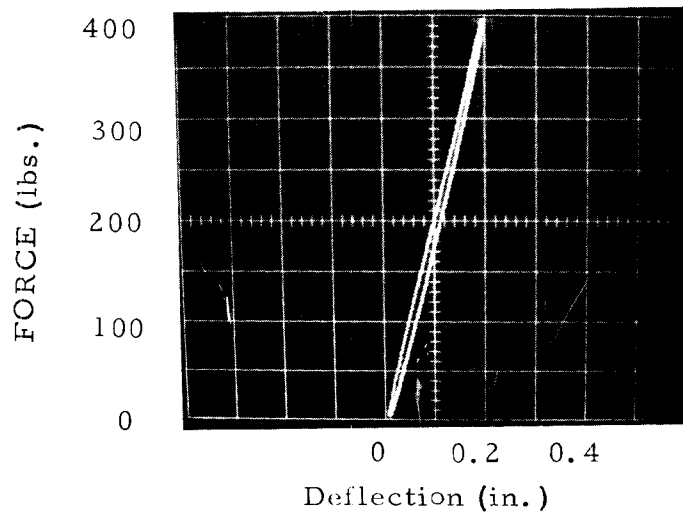


FIGURE 15c
PARAMOUNT FRAME
2000 lbs/in

FIGURE 15 VERTICAL HUB DEFLECTION DUE TO PEDAL LOAD

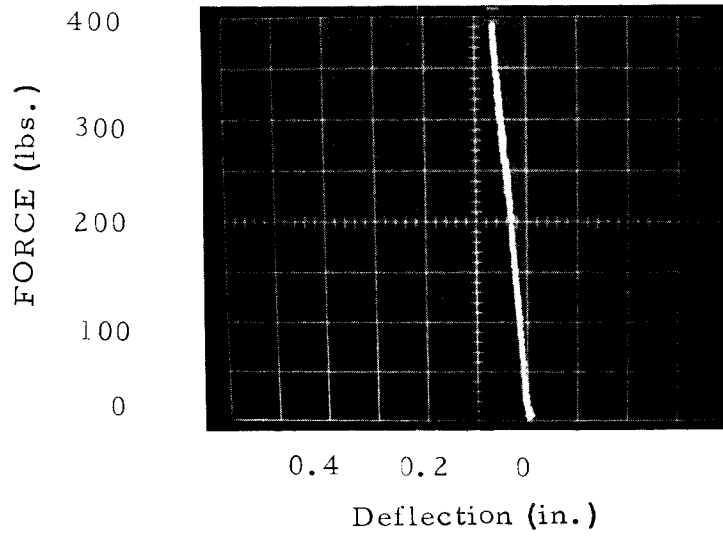


FIGURE 16a
CONTINENTAL FRAME
5700 lbs/in

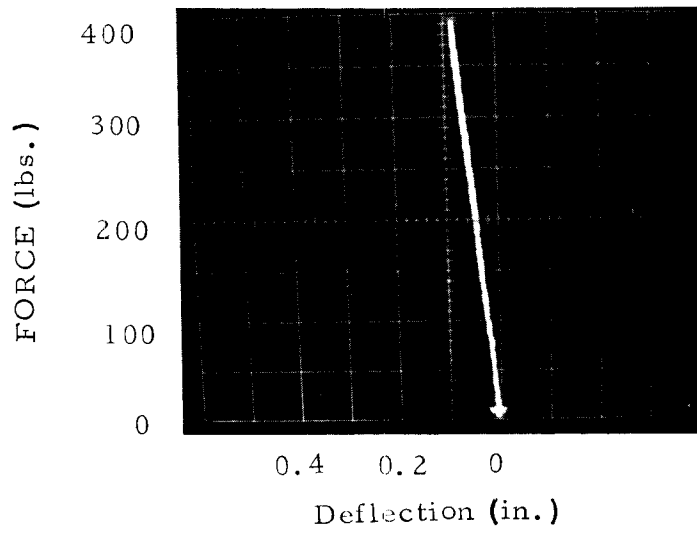


FIGURE 16b
SUPER SPORTS FRAME
4400 lbs/in

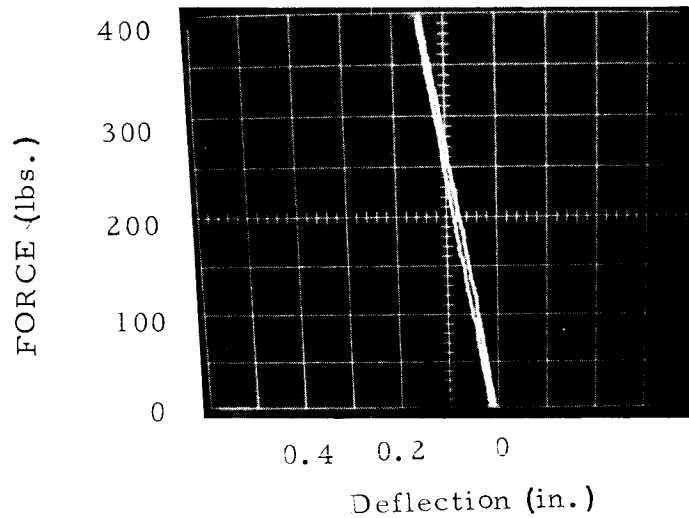


FIGURE 16c
PARAMOUNT FRAME
2700 lbs/in

FIGURE 16 LATERAL HUB DEFLECTION DUE TO PEDAL LOAD

	<u>Stiffness Coefficient (lbs/in)</u>	
	<u>Vertical</u>	<u>Lateral</u>
Continental	2900	5700
Super Sports	3300	4400
Paramount	2000	2700

Here again, the Paramount frame was significantly more flexible than either of the other frames. Of further interest is the comparison of the Continental and Super Sports data. The Super Sports frame is slightly stiffer vertically, but the Continental frame is stiffer laterally. This may be due in part to the heavier lower rear stays on the Continental.

The analysis of heat energy losses in these tests would have been aided by an expanded deflection scale. Unfortunately, the amplifier used in conjunction with the linear potentiometer was limited to the scale shown. Firm conclusions cannot be drawn based on this data, but a noticeable energy loss appears to be indicated in the Paramount data of Figures 15c and 16c.

5.0 CONCLUSIONS AND RECOMMENDATIONS

In summary, the major results of this study are the following:

- The frame tests showed the Paramount frame to be considerably more flexible than either the Continental or the Super Sports frame. In two out of the three cases observed, the Continental and Super Sports frames exhibited similar force vs. deflection characteristics.
- Little difference in stiffness was observed between the Super Sports and Paramount front forks.
- For the pedal load ranges tested, the frames were found to be essentially elastic.
- A mechanism was described for the return of energy stored in the frames as a result of flexure into useful tractive energy. The amount of this energy returned to propulsion was shown to be a function of rider characteristics, and to a certain extent, frame flexibility.

These initial results show that the stiffness of a frame can be directly related to its efficiency of energy utilization, but the characteristics of the rider's input forces must be better known before this efficiency can be quantified. When the rider's pedal force vs. crank angle function is determined, the analyses described herein can be used to compare the energy efficiencies of various frame designs. The study of the rider's bicycling characteristics could be done together with energy measurements of the bicycle under actual pedalling conditions. Valuable information could be gained through the measurement of different bicycles and the comparison of their input and output energy characteristics under such conditions.

The relationship of frame properties to energy use is only part of the question of bicycling efficiency. Also of importance is the rider's ability to utilize a certain bicycle's design characteristics and the importance of efficiency/weight ratio in various modes of bicycling. If coefficients could be determined for the efficiency of various frames, then analyses could be made of the comparative energy utilization of different bicycles over typical riding conditions including various riding speeds, grades, and accelerations.